Published in final edited form as:
Mol Pharm. 2012 April 2; 9(4): 734–743. doi:10.1021/mp2004109.

Mapping Site-Specific Changes that Affect Stability of the N-Terminal Domain of Calmodulin

Mary E. Krause, **Talia T. Martin**, and **Jennifer S. Laurence***
Department of Pharmaceutical Chemistry, University of Kansas, Lawrence, KS 66047

Abstract

Biophysical tools have been invaluable in formulating therapeutic proteins. These tools characterize protein stability rapidly in a variety of solution conditions, but in general, the techniques lack the ability to discern site-specific information to probe how solution environment acts to stabilize or destabilize the protein. NMR spectroscopy can provide site-specific information about subtle structural changes of a protein under different conditions, enabling one to assess the mechanism of protein stabilization. In this study, NMR was employed to detect structural perturbations at individual residues as a result of altering pH and ionic strength. The N-terminal domain of calmodulin (N-CaM) was used as a model system, and the ^{1}H-^{15}N heteronuclear single quantum coherence (HSQC) experiment was used to investigate effects of pH and ionic strength on individual residues. NMR analysis revealed that different solution conditions affect individual residues differently, even when the amino acid sequence and structure are highly similar. This study shows that addition of NMR to the formulation toolbox has the ability to extend understanding of the relationship between site-specific changes and overall protein stability.

Keywords

NMR spectroscopy; calmodulin; site-specific; pH titration; ionic strength; chemical shift perturbation; protein stability

INTRODUCTION

Maintaining the viability of a protein therapeutic depends on the ability to preserve its structural and chemical integrity during storage. Formulating a protein as a therapeutic is challenging and typically requires screening an extensive matrix of solution conditions and excipients to identify the composition that most effectively maintains the native state of the protein. High-throughput screening using a complement of spectroscopic and calorimetric techniques has enabled rapid evaluation of protein stability to help identify potential formulation conditions. The techniques commonly employed in the screening process report on global features of the protein. For example, circular dichroism (CD) is used to determine retention of secondary structure elements and intrinsic and extrinsic fluorescence studies are used to probe accessibility of hydrophobic surface area, reflecting compactness of the tertiary fold.[2–5] Despite an enormous number of proteins having been analyzed, clear trends have not emerged that enable one to predict which aspects of a formulation enhance stability

*Author to whom correspondence should be addressed: Jennifer S. Laurence: Telephone (785) 864-3405; Fax (785) 864-5736; laurencj@ku.edu.

SUPPORTING INFORMATION AVAILABLE

NMR spectral overlays and plots depicting changes in peak position for varied ionic strength and pH conditions. This material is available free of charge via the Internet at http://pubs.acs.org.

for an individual protein.[6] Understanding how different components in a formulation influence a protein's stability would be useful in providing a path toward rational design. NMR spectroscopy has the ability to provide such molecular detail, because it can be used to detect structural perturbations that occur at individual residues within a protein under a range of conditions, such as varied pH, ionic strength and/or excipient concentration. Determination of the specific residues impacted by a given change in solution conditions can provide insight into the mechanisms of protein stabilization and destabilization, particularly when paired with biophysical approaches that quickly assess overall stability of a protein.

Solution NMR spectroscopy is a valuable tool for studying changes in structure, conformation, and dynamics. The ^{1}H-^{15}N HSQC experiment is commonly used to examine proteins because it detects the NH group from each residue and provides information about the local backbone environment throughout the protein. NMR reports on the chemical composition of a molecule but it is exquisitely sensitive to local conformation and dynamics such that the chemical shift reflects the average bond angle. Therefore, if the angle or the timescale of motion is altered, that change is reflected in the spectrum. In addition, it is possible to assign each peak to an individual residue and assess site-specific conformational changes. For example, the chemical shift positions for the apo and holo forms of calmodulin are radically different despite very small changes in secondary and tertiary structure.[7,8] Additionally, the changes in the dynamics/flexibility of the protein in solution may also be assessed by monitoring the broadening or sharpening of a peak that may occur as a consequence of changing the solution conditions.[9,10] While it is possible to examine dynamical properties in fine detail, general hallmarks can also be used to quickly identify that the protein's conformational behavior is altered. NMR provides a unique approach to analyze both local structure and overall conformational changes, serving as a complimentary tool to other spectroscopic techniques that evaluate molecular mechanisms of physical stability.

Calmodulin (CaM) is a well-characterized calcium-sensing protein found in many organisms, and it is commonly used as a model system in the development of methods to study proteins.[811–13] The structure, Ca^{2+} binding properties, and chemical and physical stability of the intact protein and its isolated domains are well established.[8,11,14–20] The sequence of CaM is highly conserved amongst organisms and is very acidic (pI ~ 4). CaMs from different organisms have similar biochemical and physical properties, as demonstrated by various spectroscopic studies.[8,13,15] CaM belongs to the EF hand family of calcium-binding proteins. The EF hand is a 12-residue, helix-loop-helix motif in which every other residue acts as a ligand to a central Ca^{2+} ion.[7] These six residues coordinate Ca^{2+} in a pentagonal bipyramidal arrangement, and CaM contains four Ca^{2+}-binding loops of similar sequence. The well-known dumbbell structure of CaM is composed of two homologous globular domains, known as the N- and C- domains, separated by a short, flexible α-helical linker.[18,21–23] Each domain is made up of two homologous structural units, resulting in C2 symmetry, and each half-domain binds a single calcium ion.[21] The N-terminal domain contains Ca^{2+}-binding sites I and II, which are 58% identical in sequence. Figure 1 shows the N-terminal domain, where the loops of the Ca^{2+}-binding sites I and II are shown in red and blue, respectively. The holo form is rigid and structurally compact compared to the highly dynamic apo form.[7,21] Both domains display low millimolar affinities for calcium.[13] Nonetheless, calcium coordination dramatically improves the structural stability of each domain.[16,17] In addition, increased ionic strength also imparts thermal stabilization to fulllength CaM and the isolated domains.[15] The isolated domains of CaM are known to remain functional and well structured even out of the context of the whole protein.[19]

Here, we use the apo form of the N-domain of $CaM_{1–76}$ (N-CaM) as a model system to probe how individual residues within the protein respond to changes in pH and ionic

strength. N-CaM is a good model system for this investigation because the protein contains no histidine or cysteine residues that may be potentially altered by pH titration. Moreover, solution NMR data indicates the calcium binding loops are disordered and highly flexible and the negatively charged residues are surface accessible[22] making their side chain carboxylate moieties unlikely to have perturbed pKa values above the normal range of 3.4–4.5.[24] Two-dimensional NMR spectroscopy was used to monitor perturbations in the backbone amides at individual residues that result from differences in solution environment, revealing residue-specific contributions to the overall structural stability of N-CaM.

EXPERIMENTAL

Materials

Calcium chloride dihydrate was purchased from Acros Organics (Fair Lawn, NJ). Potassium chloride, Tris(hydroxymethyl)aminomethane hydrochloride (Tris-HCl), 4-(2-hydroxyethyl)-1-piperazineethane-sulfonic acid (HEPES), 3-(4-morpholino)propane sulfonic acid (Mops), 2-(4-morpholino)ethanesulfonic acid (MES), ethylenediamine tetraacetic acid disodium salt dihydrate (EDTA), and sodium chloride were all purchased from Fisher Scientific (Pittsburg, PA). For NMR experiments, ^{15}N-ammonium chloride and deuterium oxide (D_2O) were purchased from Cambridge Isotope Laboratories (Andover, MA).

Cloning and Construction of the Expression Plasmid

The full-length cDNA of calmodulin was subcloned into the pET-15b plasmid as described by previous methods (gift from J. Urbauer).[25] Although the DNA obtained encodes the gene from chicken CaM, *Xenopus laevis* CaM has an identical amino acid sequence.[13] The N-terminal domain of calmodulin was obtained by using the PCR-based QuikChange method (Stratagene) to mutate K77 within full-length CaM to a stop codon. The following primers were used to generate N-CaM coding region: 5’-gatggcaagaaaaatgtaagatacagatagcgag-3’ and 5’-ctcgctatctgtatcttacatttttcttgccatc-3’. PCR products were digested at 37 °C with Dpn I (Promega) for 1.5 hours. Immediately after digestion, the DNA was transformed into XL-1 Blue Competent cells (Stratagene) and spread on LB agar plates containing 100 mg/L ampicillin, then incubated at 37 °C overnight. Colonies isolated from the plates were cultured overnight at 37 °C in LB with ampicillin. The plasmid DNA was isolated and purified using Qiagen Spin Miniprep Kit (Stratagene). Incorporation of the taa stop codon after residue M76 was confirmed by sequencing the DNA using the T7 promoter and T7 terminator primers (Northwoods DNA, Inc., Bemidjii, MN).

Expression of N-CaM in *E. coli* cells

The pET-15 plasmid containing the gene for N-CaM was transformed into BL21 (DE3) cells (New England Biosciences, Ipswich, MA), plated on LB/amp plates, and grown overnight at 37 °C. Starter cultures were made by inoculation with a colony into 20 mL of LB containing ampicillin and grown overnight at 37 °C and 250 rpm. To obtain ^{15}N-labeled protein for NMR analysis, N-CaM was expressed in M9 minimal media containing ^{15}N-labeled ammonium chloride. Starter cultures were added to Fernbach flasks containing 1 L of minimal media, and cells were grown to an optical density at 600 nm (OD_{600}) of 0.6–0.8 before induction with a final concentration of 1 mM of isopropyl β-D-1-thioglactopyranoside (IPTG) (Acros Organics). Upon induction, supplemental calcium was added to a final concentration of 1 mM $CaCl_2$. Cells were harvested after 4 additional hours of growth by centrifugation at 4,500 × *g*, and cell pellets were stored at −80 °C. Expression of N-CaM was verified with non-reducing 16% tris-tricine SDS-PAGE.[26]

Purification of N-CaM

Cell pellets containing the overexpressed N-CaM were resuspended in 250 mM MOPS at pH 7.5, 100 mM KCl, 1 mM DTT, 1 mM EDTA and lysed by a French Press at 20,000 psi. Cellular debris were removed via centrifugation, and the lysate containing the soluble N-CaM was added to an equal volume of the lysis buffer containing $CaCl_2$ bringing the calcium concentration to 10 mM. The lysate was applied to a phenyl sepharose column (GE Healthcare), attached to an Äkta Explorer System (GE Healthcare), equilibrated with 50 mM Tris-HCl, pH 7.4, containing 10 mM $CaCl_2$ and 500 mM NaCl. The column was washed with an additional 100 mL of loading buffer before a 100 mL gradient of 0 to 100% elution buffer (50 mM Tris-HCl, pH 7.4, containing 10 mM EDTA) was run to separate any nonspecifically bound proteins. CaM eluted after one column volume of the low salt, EDTA-containing elution buffer, due to the decrease in exposed hydrophobic surface area that occurs in N-CaM upon release of the bound calcium.[27] Protein fractions were collected in tubes containing an equal volume of 100 mM MES at pH 5.5 and 100 mM $CaCl_2$, to immediately stabilize the protein. Fractions containing N-CaM were concentrated to 1.5 mL using an Amicon Ultra concentrator (Millipore) with a 3.0 kDa molecular weight cutoff and the sample applied to a Superdex 75 10/300 GL column (GE Healthcare) equilibrated in 20 mM MES, pH 5.5, containing 100 mM $CaCl_2$. The chromatographic separation was monitored by UV absorption at 220 nm, and the pure N-CaM was eluted in 5 mL fractions. The purity of fractions containing N-CaM were identified by 16% tris-tricine SDS-PAGE[28] to obtain >95% purity and the protein was again concentrated. Because N-CaM possesses no tryptophan or tyrosine residues, the absorbance of phenylalanine at 259 nm is used for quantification (ε_{259} = 975 M^{-1} cm^{-1}). Final samples were stored in the SEC buffer at 4 °C.

NMR Sample Preparation

Apo N-CaM was obtained by dialyzing 0.6 mL of concentrated holo N-CaM in a 3.5 kDa molecular weight cutoff Slide-a-Lyzer dialysis cassette (Thermo Scientific, PA) against 1 L of 10 mM MES, pH 5.5, containing 100 mM EDTA, at room temperature. Two rounds of dialysis, one hour each, were performed to remove the calcium. A pH titration of apo N-CaM was performed at pH 5.4, 5.8, 6.2, 6.5, 7.1, and 7.4. by dialyzing 0.6 mL of N-CaM against 1 L of 10 mM MES (pH 5.5 – 6.5) or 10 mM HEPES (pH 7.1 and 7.4) containing 1 mM EDTA for 2 hours. Ionic strength was adjusted with NaCl to 20 mM. Apo N-CaM was removed from the dialysis cassette, quantified by UV absorbance, and diluted for a final protein concentration of 0.2 mM. D_2O was added to a final concentration of 6% for NMR analysis. To confirm that the NMR spectra of N-CaM is not altered by the concentration of the protein, N-CaM was diluted to 0.05 mM and a spectrum collected at pH 5.4 and I=20 mM. pH 7.4 samples were also examined at 1.2 mM and 0.01 mM protein concentrations, and the spectra are unchanged.

To analyze the effect of ionic strength on the physical stabilization of apo N-CaM, ionic strength titrations were performed at three different pH values (pH 5.4, 6.2, and 7.1), using either MES or HEPES buffer containing 1 mM EDTA. Ionic strength was adjusted using sodium chloride. At each pH, samples were evaluated at 20, 40, 70, 100, 130, 160, 250, and 500 mM ionic strength. These calculated values account for all contributing ionic species, including the buffer and EDTA components at each pH. The free acid of each buffer was used, and the amount of base necessary to raise the pH from both the EDTA and the buffer component were calculated and considered when preparing each sample at the exact ionic strength specified. pH values were measured after preparation to ensure proper calculation. Equation 1 was used to determine the total ionic strength (I), in which M_i is the molar concentration of an ionic species and Z_i is the charge of that ionic species at the specific pH used.

$$I=\frac{1}{2}\sum_i M_i Z_i^2 \quad (1)$$

Samples (0.6 mL) were dialyzed into 1L of the desired solution conditions for 2 hours using 3.5 kDa molecular weight cutoff dialysis cassettes. Upon completion of each dialysis step, the pH of the sample was confirmed using an Accumet pH meter (Fisher Scientific) calibrated with 3-points at pH 4.00, 7.00, and 10.00, and the increased ionic strength values were validated by observing changes in the 90 degree pulse width, which increases proportionally with increasing ionic strength.

NMR Experiments

The ^{1}H-^{15}N HSQC experiments were performed on a Bruker Avance 600 MHz spectrometer equipped with a triple resonance probe. The spectra were acquired in 16 scans with 2048 points in ^{1}H and 128* increments in ^{15}N. An external standard, 4,4-dimethyl-4-silapentane-1-sulfonic acid (DSS), in D_2O was used for referencing the chemical shift position of ^{1}H. Indirect referencing of ^{15}N to ^{1}H was determined by using the frequency ratio method $^{15}N/^{1}H = 0.101329118$.[29] Data were processed using NMRpipe[30] and the NMR assignment program Sparky[31] was used to determine positions of peaks in the spectra acquired from the ^{1}H-^{15}N HSQC experiments. An ^{1}H-^{15}N HSQC NMR spectrum was collected and compared to previously reported NMR spectral assignments of apo CaM from *Xenopus laevis*.[8,22,23] Resonances from residues in each of the Ca^{2+}-binding loops of site I and II, the adjoining beta strands, and additional residues outside of the binding sites were identified in the spectra. The appearance of characteristic high-field amide protons (9.0–10.0 ppm), corresponding to the glycine residue at the sixth position of each of the two Ca^{2+}-binding loops, indicates the apo form is well structured. This structural and spectral feature is common among properly folded, functional Ca^{2+}-binding proteins within the EF hand family.[8] CaM is susceptible to deamidation at N60. Under the higher pH conditions used in our study, chemical degradation at this site occurs. Based on the established deamidation rate of N60 ($T_{1/2}$ = 21 days at pH 7.4, 37 °C)[32] and the well-established relationship between deamidation rate and pH[33] the amount of time each sample could be used was determined based on the set of solution conditions used. In all cases experiments were conducted such that a negligible amount of degradation occurs during the entire data acquisition period. Based on the signal to noise ratio of the NMR experiments, deamidation in excess of 5% would be detectable, but no evidence of degradation was observed. ^{1}H-^{15}N HSQC experiments used to monitor apo N-CaM at pH 5.5 at 25 °C were repeated over the course of one month and the data confirm that no spectral differences are observed in this time frame (data not shown). Changes in combined chemical shifts, in both the ^{1}H and ^{15}N dimensions, were calculated for each peak in all solution conditions, where the differences in chemical shift position between the spectrum of interest and the spectrum collected in the initial solution condition were expressed as the square root of the sum of the squares of the frequency differences (Equation 2).[34].

$$\Delta f=[(\Delta\delta\,^{1}\mathrm{H}*599.743)^{2}+(\Delta\delta^{15}\mathrm{N}*60.778)^{2})]^{1/2} \quad (2)$$

RESULTS

NMR was used to obtain site-specific information about the influence of pH and ionic strength on residues in the N-terminal domain of calmodulin (N-CaM). The stability of CaM is known to vary under different solution conditions, so NMR was used here to probe the residue-specific contributions to overall stability. A pH titration of apo N-CaM was

performed over a broad pH range, beginning at pH 5.4 to minimize chemical and physical degradation during storage and analysis. Following each ^{1}H-^{15}N HSQC experiment, the sample was dialyzed to higher pH to yield a series of spectra over the pH range of 5.4 to 7.4 (Figure 2). To confirm the spectral changes at different pH and ionic strength conditions are reversible, the sample was dialyzed back to pH 5.4 and reanalyzed; the spectra appear identical, indicating the spectral changes are reversible (data not shown). By tracking the unidirectional movement of individual peaks during a titration, each chemical shift position was correlated with the reported assignments.[8,23,35] Most peaks could be assigned, as they either remained unchanged or were in portions of the spectrum free from overlap. Several residues of interest could not be identified or tracked due to peak overlap and/or extreme crowding, specifically in the center of each spectrum. Variation in the position of selected peaks provides evidence of structural perturbations at individual nuclei with varied pH, thereby demonstrating changes in local structure as a consequence of increasing the pH. The majority of the resonances of individual residues undergo only minor shifts with varied pH; this lack of change in chemical shift positions indicates that the global structure is not affected over the course of the titration. Conversely, a few individual peaks are affected considerably. Specifically, chemical shift positions of individual residues within site II varied as a function of pH, indicating site II undergoes a local structural and/or dynamic change in response to altered pH.

The peaks circled in Figure 2 correspond to individual residues that undergo relatively large changes in chemical shift position with changing pH. N60, G61, and D64, located in binding site II, display the largest change and move substantially upfield with increasing pH. Peaks corresponding to other, even adjacent, residues are not substantially altered by pH. Large variations in chemical shift position for only a small subset of residues indicate that pH disproportionately affects Ca^{2+}-binding site II.

The equivalent residues in binding site I to those perturbed in site II are impacted less by pH. Because they are in equivalent structures, one would expect similar changes in chemical shift or resonance frequency *(Δf)* as a function of pH. Comparison of the chemical shift changes as a function of pH in sites I and II reveal their behavior differs (Figure 3). Residues in site I do not display as large of changes in chemical shift position as observed for the analogous residues in site II. Changes in site I are more comparable to changes observe throughout the rest of the fold during the pH titration; while the Δf for residues in binding site II varies up to 375 Hz, deviations from the original peak positions in site I are less than 100 Hz. Thus, the local conformational changes are more pronounced in site II compared to the residues in binding site I. Residue D64 is positioned in the short β-turn structure of binding site II. A large chemical shift deviation is observed for this residue. The corresponding residue in site I is T28. The peak corresponding to T28 is partially overlapped with I27 and its Δf cannot be determined accurately; nonetheless, it is clear that, like the rest of binding site I, T28 does not undergo nearly as large a shift in peak position as D64. Additional residues located in the turn and adjoining helix of each binding site were also examined. Plots of these residues show much smaller Δf values (supporting information).

^{1}H-^{15}N HSQC experiments were performed to assess how ionic strength affects individual residues in apo N-CaM. High ionic strength is known to enhance the thermal stability of N-CaM,[12,15] but the molecular mechanism of stabilization is not known. To determine which portions of N-CaM are affected by increasing ionic strength (*I*), an ionic strength titration was conducted. This was accomplished by comparing a series of ^{1}H-^{15}N HSQC experiments over the range of 20 – 500 mM ionic strength. The spectral overlay of the ionic strength titration performed at pH 5.4 shows peaks from residues in site I and site II are perturbed (Figure 4). G25 and G61 as well as D64 undergo the largest changes, shifting by more than 200 Hz over this range of ionic strength, while neighboring residues G23–D24 and G59–

N60 are impacted much less (Figure 5). NMR spectra were collected at three different pH values (pH 5.4, pH 6.2 and pH 7.1) to assess to the degree to which ionic strength changes are affected by the pH of the sample (spectral overlays are shown in SI: Figures S1 and S2). Peak positions were identified, and peak movement (Δf) was plotted as a function of increasing ionic strength for the titration at each pH (Figures 5–7). The peak position for G25 migrates to a higher chemical shift value in response to both increasing pH and ionic strength, which is manifest in a narrowing of the chemical shift range over the ionic strength titration with increasing pH. The largest changes in position for this residue are observed at low ionic strength values in the different pH spectra and the least amount of change in position among the different pH samples occurs at the highest ionic strength (Figures 8–9, S3). G61 moves to a higher chemical shift position in response to increasing ionic strength and pH, but the impact of ionic strength on peak position is smaller than that of pH. D64 also shifts toward higher ppm values with increasing pH and ionic strength, and the Δf appears similarly affected by both parameters.

At each of the ionic strength conditions tested, changing the pH alters the chemical shift positions in both sites and specific residues in each site are disproportionately perturbed compared to most of the protein. The loop residues in site II are greatly impacted by changing pH, whereas analogous residues in site I are impacted to a lesser extent. Not all residues in these loops are perturbed by titrating pH or ionic strength, but D22 is affected by ionic strength to a great extent than D56 in the analogous position in site II, and D22 is more dramatically altered by ionic strength at higher pH (See SI Figure S5). While the majority of large changes occur in the calcium-binding loops, some of the peaks affected correspond to residues involved in more structured elements of the EF hand, including those that participate in forming the short beta turns (T26–T28, T62–D64) (See SI Figures S4 and S5). The chemical shift position of T26 in site I changes much more than T62 in the analogous position in site II. The chemical shift of T26 is increasingly sensitive to ionic strength at higher pH, while no alteration is observed for T62 over the pH range examined. Differences in chemical shift positions for I27 and T28 cannot be quantified due to overlap. Qualitatively, there appears to be little difference in the extent to which I27 and I63 are affected by ionic strength. Substantial changes in peak position are observed for D64 while T28 remains largely unperturbed. T29 and F65 are positioned at the N-terminal end of the adjoining helix, and neither residue is altered in response to changing solution conditions. Residues in the central helices are largely unaffected by changing the pH and ionic strength (Figures 3, 5–8) indicating that the effects of the solution environment are experienced mostly at the calcium-binding loops and adjacent beta turns rather than throughout the molecule and its core. Interestingly, the loop located on the opposite face of the domain also is not perturbed upon titrating the pH or ionic strength, despite also being flexible and surface accessible (See SI Figure S6).

DISCUSSION

Here we present the use of NMR spectroscopy to identify specific residues that are affected by systematically changing solution conditions. The 2D ^{1}H-^{15}N HSQC experiment was employed to detect perturbations that occur to the backbone amide moieties at individual residues as a result of titrating pH and/or ionic strength. The apo form of the N-terminal domain of calmodulin was used as a model system because it is composed of two homologous structural units, permitting simultaneous investigation of global and local structural effects.

A pH titration of N-CaM monitored by 2D NMR revealed small overall conformational adjustments occur throughout the protein, while large changes are observed for a subset of individual residues, specifically N60, G61, and D64 within Ca^{2+}-binding site II. The

structure of Ca^{2+}-binding site II is analogous to site I, as observed in both the high-resolution structures of CaM and the unique chemical shifts in the NMR spectra for residues in comparable positions.[21,35] Nonetheless, despite having the same fold and high sequence identity (58%),[18,35] residues in structurally equivalent locations are affected differently by the solution environment, as large perturbations to residues in site II are observed in the NMR, while changes in site I are smaller. Chemical shift changes either indicate direct binding or reflect differences in conformational averaging,[36] either of which could influence the structural and thermal stability of the protein.

Pharmaceutical formulations of proteins often include ionic compounds to help stabilize proteins in aqueous solutions;[33] ions are used in these formulations to increase solubility and thermal stability of a protein in aqueous solution.[6,33] The thermal stability of N-CaM has been previously reported and the melting temperature (T_m), as measured by CD varies with different solutions conditions.[37,15] O'Donnell *et al.* reported that the T_m of the N-terminal domain at pH 7.4 is increased by 2.6 °C in 100 mM KCl, and by an additional 3.9 °C in 300 mM KCl, demonstrating the stability of N-CaM is improved with increased ionic strength.[12] Wang *et al.* measured the T_m of CaM at pH 7 and varied the KCl concentration from 0–500 mM.[38] We plotted the change in T_m as a function of KCl concentration and compared the curve to the change in peak position (Δf) as a function of ionic strength obtained using our pH 7.1 NMR titration data. The curvatures of the plotted data closely parallel each other (See SI Figure S7). While the NMR data show that changing the ionic strength has minimal impact on the majority of the backbone of N-CaM, indicating the average overall conformation is largely unaltered, the presence of large deviations specifically at site II further supports that this loop may be a determinant of structural stability. Taken together, these suggest that the site-specific changes observed in site II in the NMR data reflect the overall thermal stability of the protein. It is interesting that residues 40–44 in the loop located on the opposite face of the domain are perturbed to a minimal extent and the Δf are comparable to the rest of the protein, including residues embedded in helical structure. These distal loop residues, like those in sites I and II, are highly solvent accessible, indicating that additional features, such as dynamics and chemical composition are critical determinants that influence stability.

There are several possible mechanisms by which chemical shift changes may be induced. Direct binding of a small molecule to a specific site on the surface of N-CaM could occur, such that the affected residues experience a perturbation.[36] Weak binding ligands induce chemical shift perturbations that are detectable with the HSQC experiment. The well-known approach known as SAR by NMR relies on this phenomenon to facilitate rationale drug design for protein targets.[39] If site-specific counterion binding is responsible for the observed spectral changes, then it would be expected that amides closest to the site of interaction would be most perturbed. If a cation were to interact weakly with the side chains in a manner that emulates Ca^{2+}-binding, then spectral changes similar to holo CaM would be anticipated. The spectrum of Ca-bound N-CaM (data not shown) is distinct from the apo form. Several peaks from site I, including D22, G25, T26 and I28, move in the general direction toward the corresponding chemical shifts in the holo state, but to a limited extent. Moreover, the other peaks from residues involved in calcium binding do not shift, including the analogous residues in site II. Based on the current data set, direct interaction cannot be confirmed but would at best involve a specific subset of residues that participate in Ca^{2+} ligation. Binding to these loops by an anion would not be expected because the sequence contains multiple negative charges that would repel a like charge from approaching.

It has been reported that buffers can alter the dynamics of proteins on the microsecond to millisecond timescale. Human liver fatty acid binding protein was examined by solution NMR and it was reported that the concentration of MES buffer altered the chemical shift

positions of a subset of residues.[40] The protein samples were examined at a single pH of 5.5 but the increasing amount of buffer concomitantly elevates the ionic strength of the samples, likely causing the observed chemical shift perturbations. The protein was also examined using bis-tris at pH 5.8. The same peaks were affected by increasing the buffer concentration, but the extent to which the chemical shifts were changed was reduced. Based on these data, the authors suggested that a weak, site-specific interaction between the buffer and protein had occurred. Examples of selective ion pairing have been reported in the literature. For example, crystal structures of hen egg white lysozyme (HEWL) demonstrate site-specific binding of anions can occur at the protein's surface.[41–44] Recently, a study performed using dilute salt solutions showed that anions can bind to the surface of HEWL in solution as well.[45]

Alternatively, addition of ions alters the bulk dielectric value of the solution and this may influence the magnetic field experienced by nuclei at the surface of the protein. Because the HSQC directly probes NH nuclei, small systematic deviations would be anticipated for all surface accessible groups in this case. The titration spectra show the majority of peaks are perturbed to a small extent and move uniformly to higher ppm values in response to the systematic change in bulk solution. This mechanism cannot, however, account for the large site-specific perturbations observed in the data sets. Lastly, hydration of the protein may be altered upon changing the solution environment such that the protein's conformational dynamics are perturbed at particular sites. If the structure and/or dynamics of water in the hydration sphere is altered, the conformation and/or dynamics of the protein would be affected indirectly by changing the properties of the bulk solvent. The exchange rate would remain fast on the NMR timescale and peaks corresponding to conformationally labile residues, such as in loops, would migrate, making this a possible explanation for the large changes in peak positions observed in our titrations.

The residues in N-CaM most affected by altering the solution conditions are surface accessible, flexible, and contain multiple acidic residues. Based on the NMR data, we conclude that the majority of the protein is affected to a small degree by bulk properties of the solution, while the calcium-binding loop, particularly site II, is affected by a different mechanism. N-CaM may experience weak interactions with cations at the Ca-binding loops or be affected indirectly as a result of changes in hydration that alter the conformation and/or dynamics of the loops in site II and to a lesser extent site I. More sophisticated studies to characterize structural and dynamical changes that result from altering the solution conditions as well as mutagenesis studies to probe individual side chain contributions would help further clarify the mechanisms responsible for the observed changes.

CONCLUSION

^{1}H-^{15}N NMR experiments were used as an investigative tool to acquire molecular information about the residues impacted by changing pH and ionic strength. The data from a series of spectra collected during pH and ionic strength titrations demonstrate that the solution environment can impact residues within highly similar sequences and analogous structural elements in different ways. In N-CaM, large perturbations occur to residues located in Ca^{2+}-binding site II, but not to the homologous site I. As such, it is evident that bulk solution conditions affect local structure and that small changes in local structure strongly impact overall stability. This study demonstrates that solution NMR can be used to identify residues impacted by the solution environment. Comparison of the changes in peak position to changes in melting temperature as a function of ionic strength suggests perturbations in site II correspond to CaM's overall structural stability. The ability to obtain such data provides a path to designing more stable proteins and improved formulations.

Supplementary Material

Refer to Web version on PubMed Central for supplementary material.

Acknowledgments

We thank Drs. Asokan Anbanandam and Andria Skinner for their technical assistance with NMR, and Emily Haynes for technical assistance. TOC figure was generated from PDB entry 1DMO. Funds were provided by the KU GRF and NIH Grant Number P20 RR-017708. MEK was funded by the PhRMA Foundation. TTM was funded by the Madison and Lila Self Graduate Fellowship.

REFERENCES

1. DeLano, WL. The PyMOL Molecular Graphics System. San Carlos, CA, USA: DeLano Scientific; 2002.
2. Mahler HC, Friess W, Grauschopf U, Kiese S. Protein Aggregation: Pathways, Induction Factors, and Analysis. J Pharm Sci. 2009; 98:2909–2934. [PubMed: 18823031]
3. Manning MC, Chou DK, Murphy BM, Payne RW, Katayama DS. Stability of protein pharmaceuticals: an update. Pharm Res. 2010; 27:544–575. [PubMed: 20143256]
4. Kelly SM, Jess TJ, Price NC. How to study proteins by circular dichroism. Bba-Proteins Proteom. 2005; 1751:119–139.
5. Fan H, Vitharana SN, Chen T, O'Keefe D, Middaugh CR. Effects of pH and polyanions on the thermal stability of fibroblast growth factor 20. Mol Pharm. 2007; 4:232–240. [PubMed: 17397238]
6. Wang W. Instability, stabilization, and formulation of liquid protein pharmaceuticals. Int J Pharm. 1999; 185:129–188. [PubMed: 10460913]
7. Biekofsky RR, Martin SR, Browne JP, Bayley PM, Feeney J. Ca2+ coordination to backbone carbonyl oxygen atoms in calmodulin and other EF-hand proteins: 15N chemical shifts as probes for monitoring individual-site Ca2+ coordination. Biochemistry. 1998; 37:7617–7629. [PubMed: 9585577]
8. Mal, TK.; Ikura, M. NMR Investigation of Calmodulin. In: Webb, GA., editor. Modern Magnetic Resonance. 2006. p. 503-516.
9. Cavanagh, J.; Fairbrother, WJ.; Palmer, AGI.; Skelton, NJ. Protein NMR Spectroscopy: Principles and Practice. Academic Press; 1995.
10. Lian, LY.; Roberts, GCK. NMR of Macromolecules: A Practical Approach. Oxford: Oxford University Press; 1993. Effects of Chemical Exchange on NMR spectra. 153–182., G. C. R.
11. Klee CB, Crouch TH, Richman PG. Calmodulin. Annu Rev Biochem. 1980; 49:489–515. [PubMed: 6250447]
12. O'Donnell SE, Newman RA, Witt TJ, Hultman R, Froehlig JR, Christensen AP, Shea MA. Thermodynamics and Conformational Change Governing Domain-Domain Interactions of Calmodulin. Methods in Enzymology. 2009; 466:503–526. [PubMed: 21609874]
13. Jurado LA, Chockalingam PS, Jarrett HW. Apocalmodulin. Physiol Rev. 1999; 79:661–682. [PubMed: 10390515]
14. Aswad, DW., editor. Deamidation and isoaspartate formation in peptides and proteins. CRC Press; 1995.
15. Masino L, Martin SR, Bayley PM. Ligand binding and thermodynamic stability of a multidomain protein, calmodulin. Protein Sci. 2000; 9:1519–1529. [PubMed: 10975573]
16. Ota IM, Clarke S. Calcium affects the spontaneous degradation of aspartyl/asparaginyl residues in calmodulin. Biochemistry. 1989; 28:4020–4027. [PubMed: 2502176]
17. Potter SM, Henzel WJ, Aswad DW. In vitro aging of calmodulin generates isoaspartate at multiple Asn-Gly and Asp-Gly sites in calcium-binding domains II, III, and IV. Protein Sci. 1993; 2:1648–1663. [PubMed: 8251940]
18. Babu YS, Sack JS, Greenhough TJ, Bugg CE, Means AR, Cook WJ. Three-dimensional structure of calmodulin. Nature. 1985; 315:37–40. [PubMed: 3990807]

19. Finn BE, Evenas J, Drakenberg T, Waltho JP, Thulin E, Forsen S. Calcium-induced structural changes and domain autonomy in calmodulin. Nat. Struct. Biol. 1995; 2:777–783. [PubMed: 7552749]
20. Tjandra N, Kuboniwa H, Ren H, Bax A. Rotational dynamics of calcium-free calmodulin studied by 15N NMR relaxation measurements. Eur. J. Biochem. 1995; 230:1014–1024. [PubMed: 7601131]
21. Chou JJ, Li S, Klee CB, Bax A. Solution structure of Ca(2+)-calmodulin reveals flexible hand-like properties of its domains. Nat. Struct. Biol. 2001; 8:990–997. [PubMed: 11685248]
22. Zhang M, Tanaka T, Ikura M. Calcium-induced conformational transition revealed by the solution structure of apo calmodulin. Nat. Struct. Biol. 1995; 2:758–767. [PubMed: 7552747]
23. Kuboniwa H, Tjandra N, Grzesiek S, Ren H, Klee CB, Bax A. Solution Structure of Calcium-Free Calmodulin. Nat. Struct. Biol. 1995; 2:768–776. [PubMed: 7552748]
24. Clark AT, Smith K, Muhandiram R, Edmondson SP, Shriver JW. Carboxyl pKa Values, Ion Pairs, Hydrogen Bonding, and the pH-dependence of Folding the Hyperthermophile Proteins Sac7d and Sso7d. J. Mol. Biol. 2007; 372:992–1008. [PubMed: 17692336]
25. Bartlett RK, Bieber Urbauer RJ, Anbanandam A, Smallwood HS, Urbauer JL, Squier TC. Oxidation of Met144 and Met145 in calmodulin blocks calmodulin dependent activation of the plasma membrane Ca-ATPase. Biochemistry. 2003; 42:3231–3238. [PubMed: 12641454]
26. Schägger H. Tricine-SDS-PAGE. Nature Protocols. 2006; 1:16–23.
27. Gopalakrishna R, Anderson WB. Ca2+-induced hydrophobic site on calmodulin: Application for purification of calmodulin by phenyl-Sepharose affinity chromatography. Biochemical and BIophysical Reserach Communications. 1982; 104:830–836.
28. Masino L, Martin SR, Bayley PM. Ligand Binding and thermodynamic stability of a multidomain protein, calmodulin. Protein Science. 2000; 9:10. [PubMed: 10739242]
29. Wishart DS, Bigam CG, Yao J, Abildgaard F, Dyson HJ, Oldfield E, Markley JL, Sykes BD. 1H, 13C and 15N chemical shift referencing in biomolecular NMR. J Biomol NMR. 1995; 6:135–140. [PubMed: 8589602]
30. Delaglio F, Grezesiek S, Vuister G, Zhu G, Pfeifer J, Bax A. NMRpipe: A multidimensonal spectra processing system based on unix pipes. J Biomol NMR. 1995; 6:277–293. [PubMed: 8520220]
31. Goddard, TD.; Kneller, DG. SPARKY. San Francisco: University of California; 2004.
32. Robinson NE, Robinson AB. Deamidation of human proteins. PNAS. 2001; 98:12409–12413. [PubMed: 11606750]
33. Wakankar AA, Borchardt RT. Formulation considerations for proteins susceptible to asparagine deamidation and aspartate isomerization. J Pharm Sci. 2006; 95:2321–2336. [PubMed: 16960822]
34. Jaren O, Kranz J, Sorensen B, Wand J, Shea M. Calcium iduced conformational switching of paramecium calmodulin provides evidence for domain coupling. Biochemistry. 2002; 41:14158–14166. [PubMed: 12450379]
35. Ikura M, Kay LE, Bax A. A novel approach for sequential assignment of 1H, 13C, and 15N spectra of Larger Proteins: heteronuclear triple-resonance three-dimensional NMR spectroscopy. Application to calmodulin. Biochemistry. 1990; 29:4659–4667. [PubMed: 2372549]
36. Skinner AL, Laurence JS. High-field solution NMR spectroscopy as a tool for assessing protein interactions with small molecule ligands. J Pharm Sci. 2008; 97:4670–4695. [PubMed: 18351634]
37. Biekofsky RR, Martin SR, McCormick JE, Masino L, Fefeu S, Bayley PM, Feeney J. Thermal Stability of Calmodulin and Mutants Studied by 1H-15N HSQC NMR Measurements of Selectively Labeled [15N]Ile Proteins. Biochemistry. 2002; 41:6850–6859. [PubMed: 12022890]
38. Wang Q, Liang K-C, Czader A, Waxham MN, Cheung MS. The Effect of Macromolecular Crowding, Ionic Strength and Calcium Binding on Calmodulin Dynamics. PLOS Computational Biology. 2011; Vol. 7:1–16.
39. Shuker SB, Hajduk PJ, Meadows RP, Fesik SW. Discovering High-Affinity Ligands for Proteins: SAR by NMR. Science. 1996; 274:1531–1534. [PubMed: 8929414]
40. Long D, Yang D. Buffer Interference with Protein Dynamics: A Case Study on Human Liver Fatty Acid Binding Protein. Biophysical Journal. 2009; 96:1482–1488. [PubMed: 19217864]

41. Walsh M, Schneider T, Sieker L, Dauter Z, Lamzin V, Wilson K. Refinement of triclinic hen egg-white lysozyme at atomic resolution. Acta Cryst D. 1998; 54:522–546. [PubMed: 9761848]

42. Vaney M, Broutin I, Retailleau P, Douangamath A, Lafont S, Hamiaux C, Prange T, Ducruix A, Ries-Kautt M. Structural effects of monovalent anions on polymorphic lysozyme crystals. Acta Cryst D. 2001; 57:929–940. [PubMed: 11418760]

43. Steinrauf L. Structures of monoclinic lysozyme iodide at 1.6 A and of triclinic lysozyme nitrate at 1.1 A. Acta Cryst D. 1998; 54:767–780. [PubMed: 9757091]

44. Lim K, Nadarajah A, Forsythe E, Pusey M. Locations of bromide ions in tetragonal lysozyme crystals. Acta Cryst D. 1998; 54:899–904. [PubMed: 9757106]

45. Gokarn YR, Fesinmeyer RM, Saluja A, Razinkov V, Chase SF, Laue TM, Brems DN. Effective charge measurements reveal selective and preferential accumulation of anions, but not cations, at the protein surface in dilute salt solutions. Protein Science. 2011; 20:580–587. [PubMed: 21432935]

A.

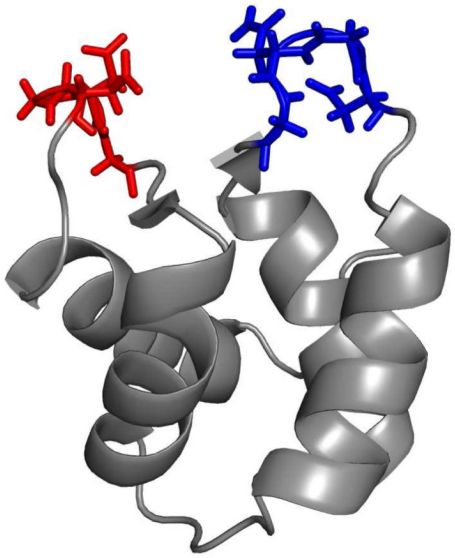

B.

	Loop						β-turn			α-helix		
Site I	D20	K21	D22	G23	D24	G25	T26	I27	T28	T29	K30	E31
Site II	D56	A57	D58	G59	N60	G61	T62	I63	D64	F65	P66	E67

Figure 1.

A. N-terminal domain of apo-calmodulin, where the loops of the calcium binding sites are shown in red (site I: D22, G23, D24, G25) and blue (site II: D58, G59, N60, G61). (PDB 1DMO). Figure generated in PyMOL.[1] **B.** Residues in the EF hand are shown in red (site I) and blue (site II). Residues that directly coordinate calcium are shaded in gray.

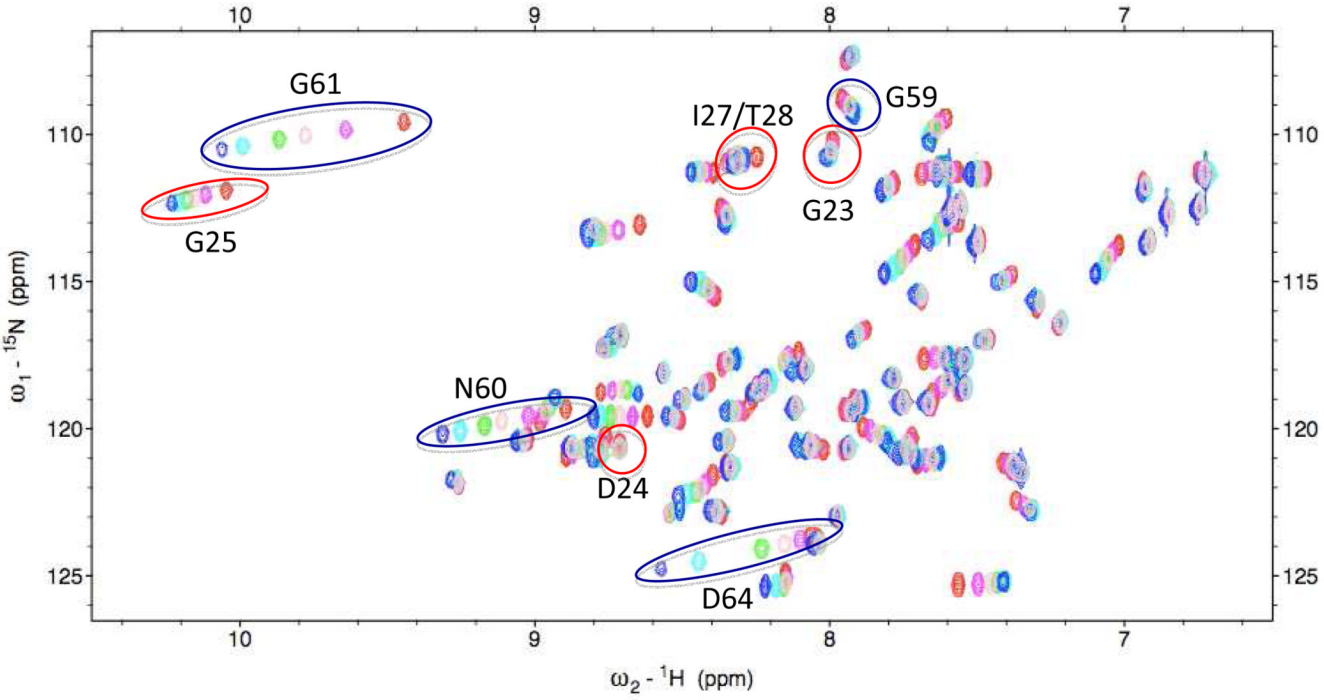

Figure 2.

A series of spectra of apo N-CaM from ^{1}H-^{15}N HSQC experiments at *I*=20 mM with increasing pH. Peaks are colored according to pH conditions: pH 5.4 (red), pH 5.8 (magenta), pH 6.2 (coral), pH 6.5 (green), pH 7.0 (cyan), pH 7.4 (blue). Selected residues in sites I (red) and II (blue) are labeled.

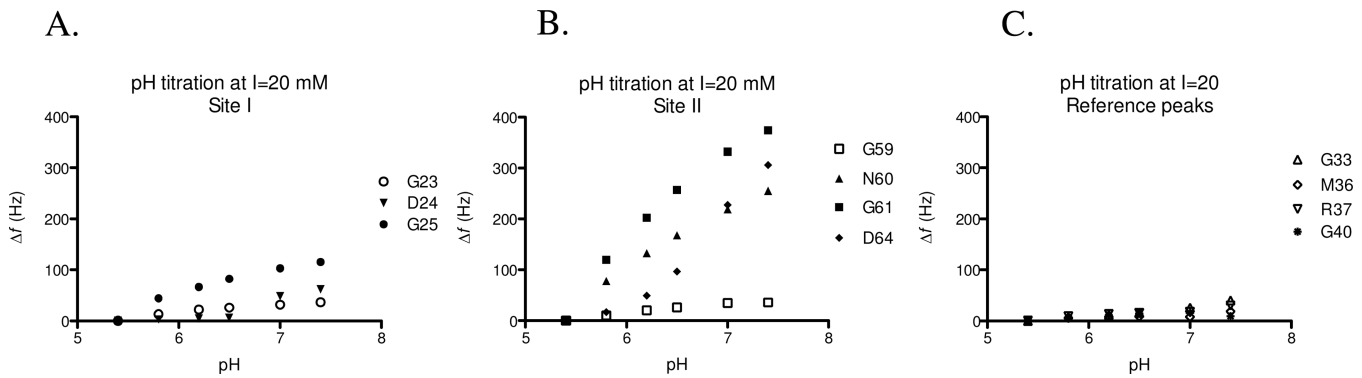

Figure 3.

Change in chemical shift position (Δ*f*) of residues in Ca^{2+}-binding loops based on ^{1}H-^{15}N HSQC spectra from the pH titration at *I* = 20 mM. Δ*f* was determined relative to peak position at pH 5.5. **A.** Residues in Ca^{2+}-binding site I. **B.** Residues in Ca^{2+}-binding site II. **C.** Residues in distant parts of the protein for reference.

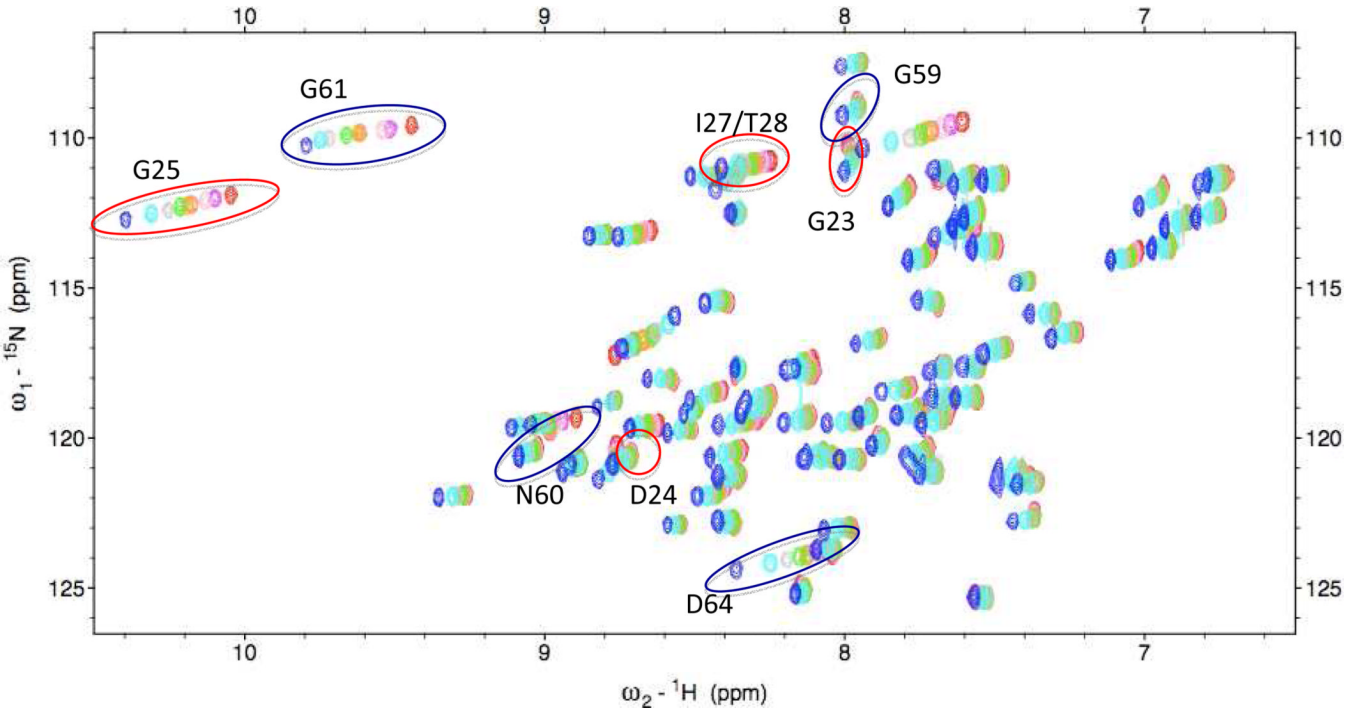

Figure 4.

^{1}H-^{15}N HSQC spectra of apo N-CaM at pH 5.4 at different ionic strength: *I* = 20 mM (red), *I* = 40 mM (magenta), *I* = 70 mM (pink), *I* = 100 mM (coral), *I* = 130 mM (orange), *I* = 160 mM (green), *I* = 200 mM (gray), *I* = 250 mM (cyan), and *I* = 500 mM (blue).

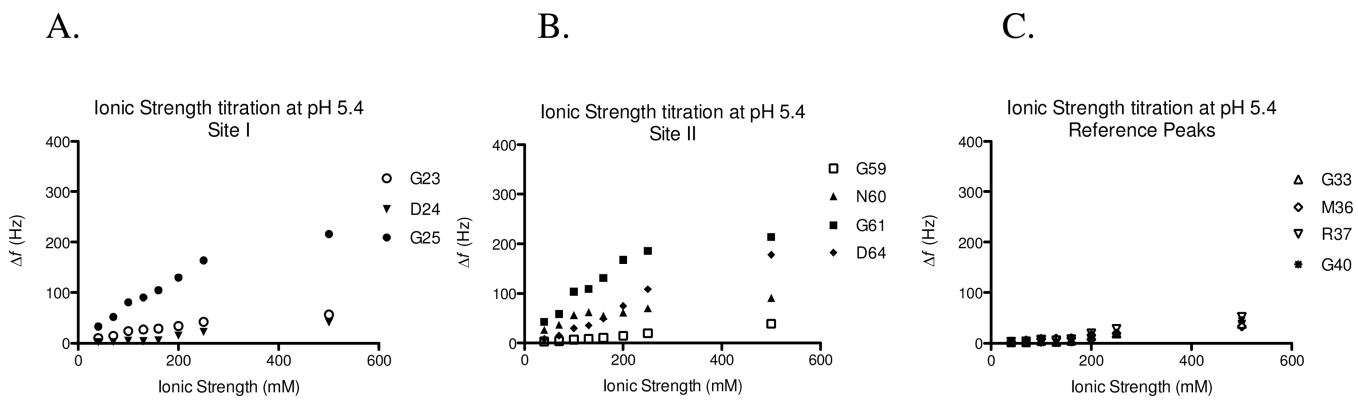

Figure 5.

Plots depict the change in chemical shift position (Δ*f*) of residues in Ca^{2+}-binding loops as a function of ionic strength at pH 5.4. The change in chemical shift is determined relative to peak position at *I*=20 mM. **A.** Residues in Ca^{2+}-binding site I. **B.** Residues in Ca^{2+}-binding site II. **C.** Residues in distant parts of the protein for reference.

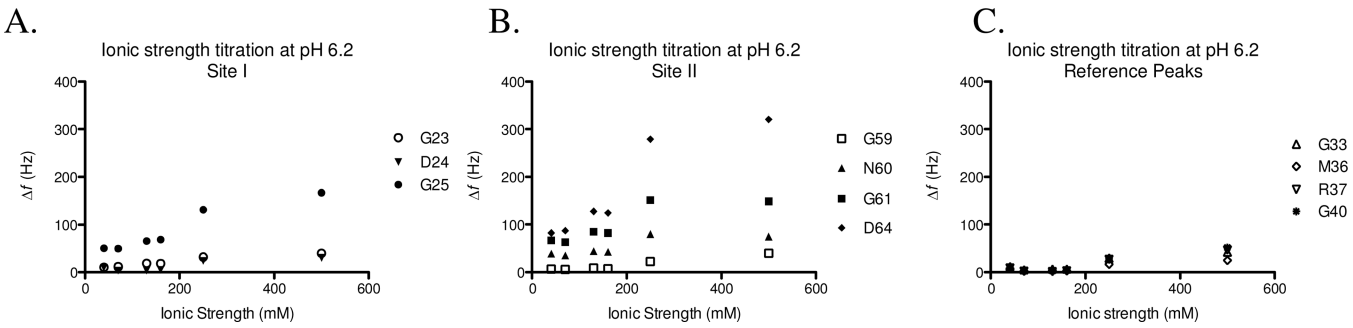

Figure 6.

Plots depict the change in chemical shift position (Δ*f*) of residues in Ca^{2+}-binding loops as a function of ionic strength at pH 6.2. The change in chemical shift is determined relative to peak position at *I*=20 mM. **A.** Residues in Ca^{2+}-binding site I. **B.** Residues in Ca^{2+}-binding site II. **C.** Residues in distant parts of the protein for reference.

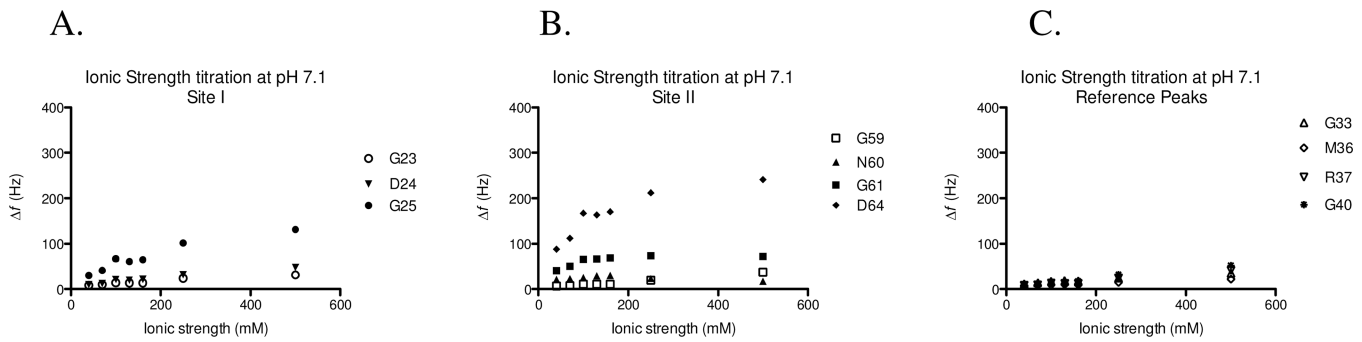

Figure 7.

Plots depict the change in chemical shift position (Δ*f*) of residues in Ca^{2+}-binding loops as a function of ionic strength at pH 7.1. The change in chemical shift is determined relative to peak position at *I*=20 mM. **A.** Residues in Ca^{2+}-binding site I. **B.** Residues in Ca^{2+}-binding site II. **C.** Residues in distant parts of the protein for reference.

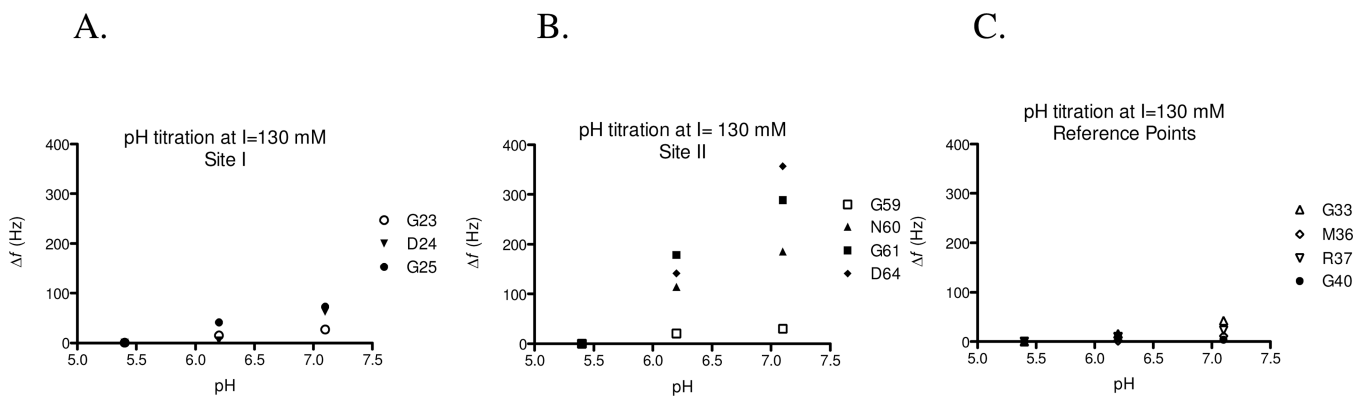

Figure 8.

Plots depict the change in chemical shift position (Δ*f*) of residues in Ca^{2+}-binding loops as a function of pH at *I*=130 mM. The change in chemical shift is determined relative to peak position at pH 5.4. **A.** Residues in Ca^{2+}-binding site I. **B.** Residues in Ca^{2+}-binding site II. **C.** Residues in distant parts of the protein for reference.

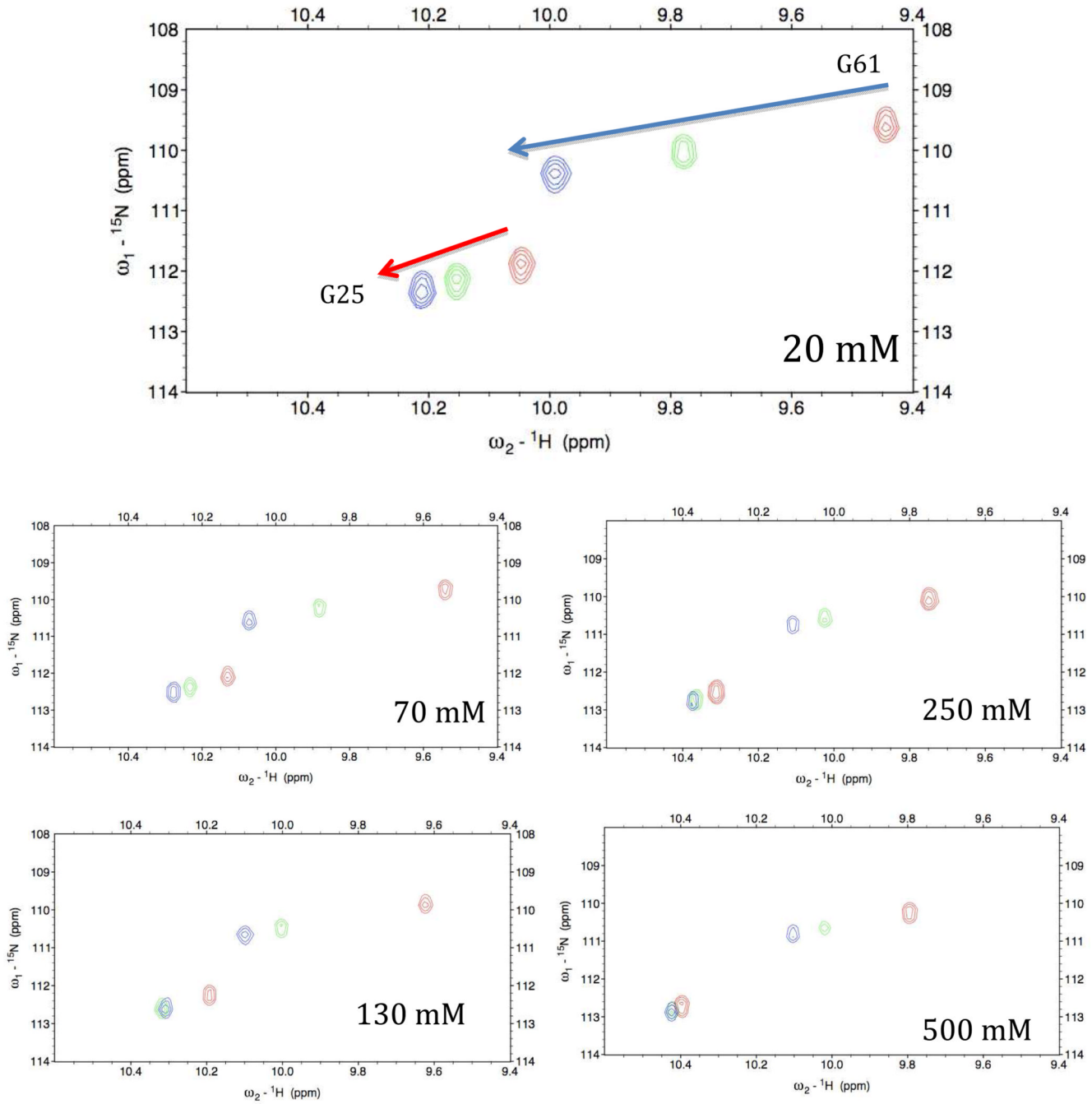

Figure 9.

G25 (site I) and G61 (site II) in a series of ^{1}H-^{15}N HSQC spectra of apo N-CaM, where site II is impacted by changing pH even at high ionic strength. In each panel, pH 5.4 = red, pH 6.2 = green, and pH 7.1 = blue. Ionic strength of each titration is shown in the lower right corner of the panel.